

Fuzzy logic direct torque control of induction motor for photovoltaic water pumping system

Aicha Belgacem¹, Yahia Miloud², Mohamed Mostefai², Fatima Belgacem¹

¹Electrical Engineering Laboratory, University of Saida, Saida, Algeria

²Geometry, Analysis, Control and Applications Laboratory, University of Saida, Saida, Algeria

Article Info

Article history:

Received May 9, 2022

Revised Jun 6, 2022

Accepted Jun 24, 2022

Keywords:

Boost converter

Centrifugal pump

Fuzzy direct torque control

Photovoltaic pumping system

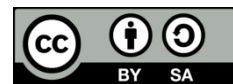
PV array

Slide mode controller

ABSTRACT

This study presents a fuzzy logic direct torque control for induction motor to be used in photovoltaic (PV) water pumping system. The system is intended to be less expensive and simple while maximizing PV array power utilization. For this purpose, a smart technology based on fuzzy logic controller (FLC) has been implemented to track the maximum power which has been successfully used in solar water pumping systems under different irradiance levels. Next, to alleviate the disadvantages of standard DTC, we chose fuzzy direct torque control (FDTC) for induction motors driving a centrifugal pump. Furthermore, this study includes the usage of IP with anti-windup and slide mode speed controller (SMC) instead of the traditional proportional-integral speed controller. Finally, the induction motor (IM) speed has been optimized with an optimum speed control in order to maximize the pump's hydraulic parameters. The FDTC, with its SMC outperforms the photovoltaic pumping system (PVPS) in terms of dynamic performance and robustness. To develop a full simulation model of the proposed PVPS configuration under various climate conditions, MATLAB environment and associated Simulink are used.

This is an open access article under the [CC BY-SA](https://creativecommons.org/licenses/by-sa/4.0/) license.



Corresponding Author:

Aicha Belgacem

Electrical Engineering Laboratory, University of Saida

Saida 20000, Algeria

Email: aicha.belgacem@univ-saida.dz

1. INTRODUCTION

Over the last several years, the globe has seen a major increase in demand for energy in all sectors of life, particularly electricity, which is obtained mainly from fossil fuels. This latter has a harmful effect on the environment. The way out of this problem is to resort to renewable energy. Many governments have implemented substantial investments in this regard and so appear to be on the right track to tackle the problem of combining energy production and consumption, while preserving the ecological equilibrium of the planet. In this instance, the sun remains the most viable energy source, whether directly or indirectly, [1].

Stand-alone water pumping systems powered by electrical motors are the most common application of photovoltaic energy. Indeed, it is the most often used energy source for supplying drinking and irrigation water in rural areas that cannot afford to connect to the national grid. Meah *et al.* [2] developed solar photovoltaic pumping systems produce appropriate amounts of clean and safe water, protecting human health and ensuring long-term development [3].

Solar modules have two primary drawbacks: a relatively high manufacturing cost and a low efficiency. As a result, the solar system must be operated at the maximum power point (MPPT) under any circumstances. Photovoltaic (PV) systems are integrated with DC-DC converters and their related control algorithms to continuously extract MPPT [4]. Strong intelligence control strategies, such as follicular

lymphoma (FL), have been developed in recent years. The key benefit of fuzzy logic control (FLC) is that it responds quickly and smoothly under a variety of solar irradiation circumstances [5]. Because of its exceptional performance in raising the efficacy of the photovoltaic pumping system (PVPS), it is being used in this attempt.

The selection of a drive system to interface with the PV source was AC induction motor (IM), because it appears to be an adequate alternative in terms of power and high PVPS reliability [6]. New controls, such as Duisburg test case (DTC), are proving to be very promising because to a variety of benefits, including simplicity, quicker response and fewer reliance on machine parameters. DTC accomplishes decoupled control of both stator flux and electromagnetic torque while the axis transformation and current regulators are not needed [7],[8]. In PV systems, DTC achieves quick responses, excellent performance and less variations in steady state for temperature variation and sudden irradiance variation, increasing the energy successfully taken from the photovoltaic generator (GPV) when compared to other types of control, especially vector control [9].

However, there are important drawbacks: the torque and stator flux ripples have a large amplitude, specially at low speeds and the switching frequency is very variable [10]. Errouha *et al.* [11] designed fuzzy logic blocks have taken the place of lookup tables and hysteresis controllers when employing adaptive fuzzy logic control for speed regulation to avoid these drawbacks. As a result, the flux and torque ripples are reduced to a minimum. Despite the fuzzy logic controller's benefits, it can achieve higher performance. The use of SMC methods instead of proportional-integral has great results and references are tracked precisely and quickly [12], that is why it is proposed to combine this control for speed regulation with fuzzy logic controller to improve the performance of DTC in this paper so that the water pumping system performs better.

The proposed system is described in Figure 1. The SMC is used to generate torque reference to deal with variations in climatic circumstances. The PV array is set to its maximum power output utilizing a boost converter with a fuzzy logic controller (FLC). In a MATLAB/Simulink environment, the starting, steady-state, and dynamic behaviours of SPWS under varying solar irradiation are studied. The paper is divided into four sections: the proposed system is designed, modeled and controlled in section 2. Section 3 discusses a comparative study and provides the simulation results. The conclusion is presented in the final section.

2. CONFIGURATION OF THE ENTIRE SYSTEM AND OPERATION

The design system, its modeling and its control are presented.

2.1. Designing a system

Figure 1 shows the global system schematic diagram constituting the motor-pump powered by PV array with fuzzy direct torque control (FDTC) while using slide mode speed controller (SMC) instead of the traditional proportional-integral speed controller. For the proper design of the PV generator (GPV) array; In order to feed a pump with induction motor drive of 1500 W with 1900 W, the GPV is constituted of two modules in parallel and five modules in series.

Regarding the pump design. The power supplied to the pump is proportional to the speed cube. For a 1435 rpm rated speed and an input power of 1.5 KW, the pump constant K_p can be calculated as, [13]:

$$K_p = \frac{P}{(\pi/30 \times N)^3} = \frac{1.5 \times 10^3}{(\pi/30 \times 1435)^3} = 0.00044 \text{ sec}^3/\text{rad}^3 \quad (1)$$

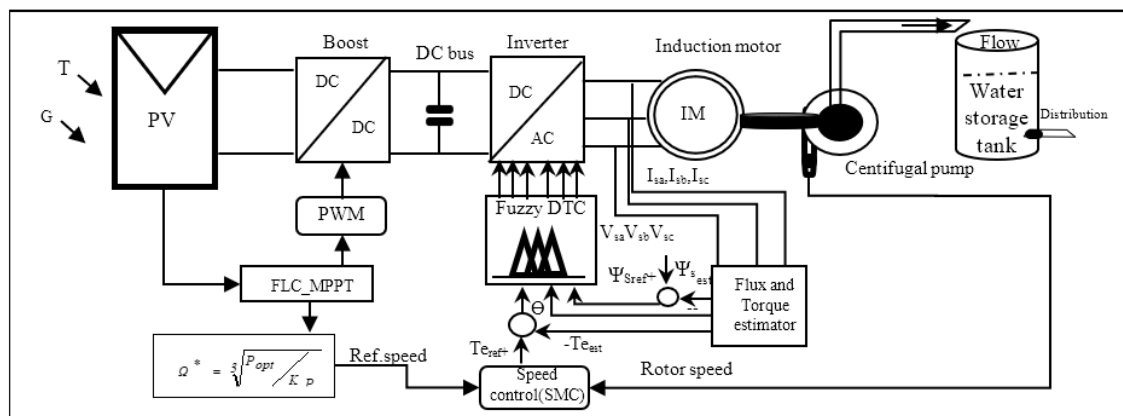


Figure 1. The global system's schematic illustration

2.2. System modeling

The following is a description of the modeling of the entire photovoltaic pumping system:

2.2.1. PV cell

It consists of a current source (I_{sc}), a diode (D), resistances (R_{sh}) and (R_s) as shown in Figure 2 [14]. The current-voltage characteristic is expressed in (2). Where I is the cell current, V is the cell voltage, n is a diode ideality factor, I_0 is the reverse saturation current of diode, q is the elementary charge, k is the Boltzmann's constant and T is the absolute temperature.

$$I = I_{sc} - I_0 \left[e^{\left(\frac{q(V+I.R_s)}{nkT} \right)} - 1 \right] - \frac{V+I.R_s}{R_{sh}} \quad (2)$$

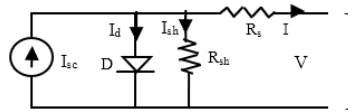


Figure 2. Circuit equivalent to a cell

2.2.2. Induction motor

The IM model is represented with these mathematical equations in the stationary frame (α, β) [15].

$$\begin{cases} \frac{di_{s\alpha}}{dt} = \lambda_1 i_{s\alpha} - p\Omega i_{s\beta} + \lambda_2 \Psi_{s\alpha} + \lambda_3 p\Omega \Psi_{s\beta} + \mu v_{s\alpha} \\ \frac{di_{s\beta}}{dt} = \lambda_1 i_{s\beta} - p\Omega i_{s\alpha} + \lambda_2 \Psi_{s\beta} + \lambda_3 p\Omega \Psi_{s\alpha} + \mu v_{s\beta} \\ \frac{d\Psi_{s\alpha}}{dt} = v_{s\alpha} - R_s i_{s\alpha} \\ \frac{d\Psi_{s\beta}}{dt} = v_{s\beta} - R_s i_{s\beta} \\ \frac{d\Omega}{dt} = \lambda_3 T_e - \lambda_5 \Omega - \lambda_3 T_p \end{cases} \quad (3)$$

The electromagnetic torque equation is:

$$T_e = \lambda_4 (i_{s\beta} \Psi_{s\alpha} - i_{s\alpha} \Psi_{s\beta}) \quad (4)$$

where $i_{s\alpha}$ and $i_{s\beta}$ are stator current components, $\Psi_{s\alpha}$ and $\Psi_{s\beta}$ are stator flux components, p is the pole's pairs number and Ω the rotor speed, $\sigma, \mu, \lambda_1, \lambda_2, \lambda_3, \lambda_4$ and λ_5 are given by:

$$\sigma = 1 - \frac{L_m}{L_s L_r}, \mu = \frac{1}{\sigma L_s}, \lambda_1 = -\left(\frac{R_s}{\sigma L_s} + \frac{R_r}{\sigma L_r} \right), \lambda_2 = \mu \left(\frac{R_s}{\sigma L_s L_r} \right), \lambda_3 = \frac{1}{J}, \lambda_4 = \frac{3}{2} p, \lambda_5 = \frac{f_v}{J}$$

with R_s and R_r are stator and rotor resistances, L_s and L_r are stator and rotor inductances, and L_m is the mutual stator-rotor inductance.

2.2.3. Centrifugal pump

The pump torque T_p which is given in (5), [16]. The hydraulic power is calculated as [17]-[19]. Where ρ, g, H and Q are respectively, the density of water, gravity, total dynamic head and water flow.

$$T_p = K_p \Omega^2 \quad (5)$$

$$P_h = \rho g H Q \quad (6)$$

3. THE SYSTEM'S CONTROL

In this section, MPPT of the GPV with FLC, SMC for speed regulator and FDTC of IM are studied.

3.1. MPPT strategies

They're getting more frequent in PV systems with non-linear characteristics these days [20]. The fuzzy MPPT control provides the optimum duty cycle (D_{opt}) to feed the converter's switch [21]. Fuzzification, inference and defuzzification are the three processes of the MPPT controller technique using FLC algorithm. Figure 3 show diagram depicts the fuzzy controller's basic structure [22].

Table 1 presents the fuzzy controller's rules, where all inputs are fuzzy sets of error ($\varepsilon(k)$) and change of error ($D\varepsilon(k)$) in (7) and (8). The output is the change of duty cycle (D) at the chopper. In the case of fuzzy control. The control rule in fuzzy control must be trained in such a way that the input variable $\varepsilon(k)$ remains zero. Where the rules are : NB, NS, PS, PB and ZE are respectively defined as negative big, negative small; positive small, positive big and zero.

$$\varepsilon(k) = \frac{P_{pv}(k) - P_{pv}(k-1)}{V_{pv}(k) - V_{pv}(k-1)} \quad (7)$$

$$D\varepsilon(k) = \varepsilon(k) - \varepsilon(k-1) \quad (8)$$

Where P_{pv} and V_{pv} are respectively the GPV power and voltage, K is the sampling time.

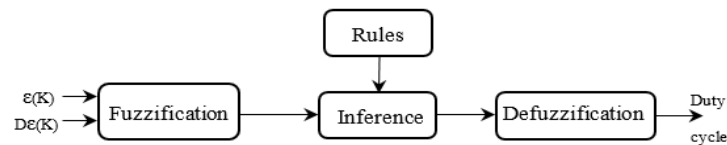


Figure 3. A fuzzy controller's general block diagram

Table 1. Table of controller's rules						
$\varepsilon(k) \backslash D\varepsilon(k)$	NB	NS	ZE	PS	PB	
NB	ZE	ZE	PB	PB	PB	
NS	ZE	ZE	PB	PB	PB	
ZE	PS	ZE	ZE	ZE	NS	
PS	NS	NS	NS	ZE	ZE	
PB	NB	NB	NB	ZE	ZE	

3.2. Fuzzy direct torque control technique description

DTC's main principle is a concept of the open-loop direct determination of the command sequence used to switch a voltage inverter in order to provide the electromagnetic torque control as well as the stator flux magnitude instantaneously. The inverter voltage vector can be expressed in the following way [23]. With I_a, I_b, I_c are switching logic states (0 or 1) while U_c is DC bus voltage. Figure 4 show diagram represents the set of voltage vectors delivered by each voltage inverter at two levels. The suggested control may be broken down into many blocks, including flux and torque estimators [24], fuzzy logic DTC, and a speed regulator.

$$V = \sqrt{\frac{2}{3}} U_c (I_a + I_b e^{\frac{j2\pi}{3}} + I_c e^{\frac{j4\pi}{3}}) \quad (9)$$

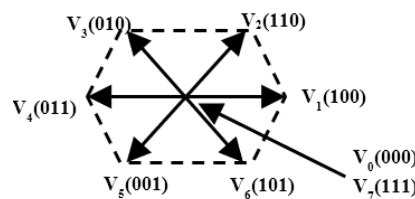


Figure 4. Voltage vectors inverter

3.2.1. DTC based on the fuzzy logic

Fuzzy logic blocks have taken the place of lookup tables and hysteresis controllers in order to improve accuracy and decrease ripples in both electromagnetic torque and flux, [24]. Figure 5 depicts the suggested controller, which is designed to provide the optimal vector required to produce the appropriate

torque and flux changes. The FDTC structure has internally three inputs and three outputs. The inputs are the electromagnetic torque error E_Torque , the stator flux error E_flux and the flux position Θ_s . The outputs are three switching magnitudes (S_a , S_b and S_c) of switches of the inverter of two levels [25], [26].

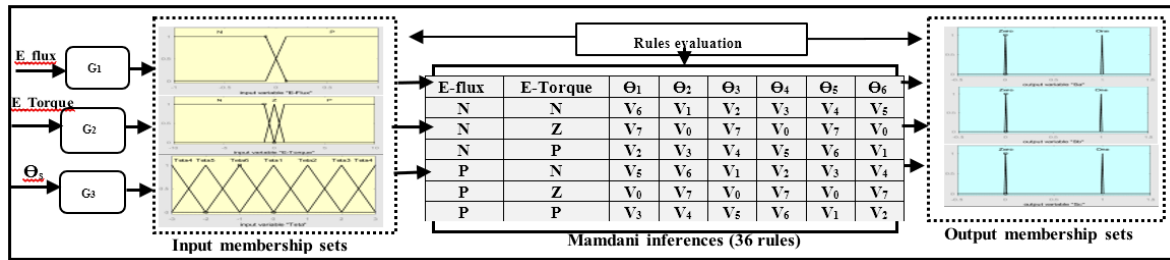


Figure 5. The proposed fuzzy controller architecture

The fuzzy controller monitors the errors signals and the sector identification angle, and changes the output voltage vector accordingly, ensuring that the electromagnetic torque and rotor flux are in line with their references [27].

$$\theta_s = \arctan\left(\frac{\psi_{s\beta}}{\psi_{s\alpha}}\right) \quad (10)$$

$$E_{Torque} = T_{eref} - T_{est} \quad (11)$$

$$E_{flux} = \psi_{sref} - \psi_{s est} \quad (12)$$

The following steps must be completed in order to design a fuzzy inference system:

- Fuzzification: The flux position discourse universe is numbered from one to six (1 to 6 fuzzy sets), for all angles θ_i the triangular membership function is used, while the electromagnetic torque error is presented in three sets (positive, zero and negative torque error (P, Z and N, respectively); for Z, we use the triangular membership function and P and N are trapezoid, in the other side, the flux error is separated into two fuzzy sets (positive and negative flux error (P and N respectively)). For P and N, we use trapezoid membership functions. Each output is divided into two sets (0 and 1), with membership functions determined by trapezoid forms.
- Fuzzy rules: Following the DTC lookup table input and output, the rules are designed. Figure 4 depicts the fuzzy rules, the output and input membership sets, the goal is to provide the controller's output variables based on the input variables [28]. Defuzzification: the simple implementation with better results led to select Mamdani technique with the Max–Min choice, which is also proven in other papers such [28].

3.2.2. The speed regulator

The first controller is composed of an IP with anti-windup loop,[29], [31]. A FDTC with the SMC was used. To increase the speed response of the IM, IP with anti-windup speed controller was substituted with SMC in this application, [30],[31]. The sliding surface is however given by:

$$\delta_1 = \Omega^* - \Omega \quad (13)$$

The surface's derivative is as follows:

$$\frac{d\delta_1}{dt} = \frac{d\Omega^*}{dt} - \frac{d\Omega}{dt} \quad (14)$$

From in (13) and (14), the derivative of the surface becomes:

$$\frac{d\delta_1}{dt} = \frac{d\Omega^*}{dt} - \lambda_3 T_e + \lambda_5 \Omega + \lambda_3 T_p \quad (15)$$

The electromagnetic torque in equation (15) is replaced by the control torque $T_{e_{ref}}$:

$$T_{e_{ref}} = T_{e_{eq}} + T_{e_n} \quad (16)$$

The (15) is transformed into:

$$\frac{d\delta_1}{dt} = \frac{d\Omega^*}{dt} - \lambda_3 T_{e_{ref}} + \lambda_5 \Omega + \lambda_3 T_p \quad (17)$$

During sliding mode, the $\frac{d\delta_1}{dt}$ and the discontinuous control T_{e_n} are both null. The equivalent control is deduced from :

$$T_{e_{ref}} = \frac{1}{\lambda_3} \left(\frac{d\Omega^*}{dt} + \lambda_5 \Omega + \lambda_3 T_p \right) \quad (18)$$

The condition of stability ($\delta_1 \cdot \frac{d\delta_1}{dt} < 0$) must be checked during the convergence mode, substituting the equivalent control (18) in (17), we get:

$$\frac{d\delta_1}{dt} = -\lambda_3 T_{e_n} \quad (19)$$

To stabilize the system T_{e_n} is chosen as follows:

$$T_{e_n} = \lambda \text{sign}(\delta_1) \quad (20)$$

Where λ is a positive gain.

4. RESULTS AND DISCUSSION:

MATLAB software is used to perform various tests to assess the studied system's performance and adaptability. Ten PV panels are used in this simulation, five are connected in series and two in parallel to get maximum power to run the motor of 1.5 kW. The PV array, the boost and the induction motor parameters are shown in appendix Table 2, Table 3, and Table 4. Different modes of operation are analyzed in order to evaluate the PVPS dynamic responsiveness under varied solar insolation levels. The irradiance and temperature are maintained at 1 kW/m² and 25 °C, respectively. The following figures show the simulation results.

Under full sunlight, the GPV generates enough power to provide complete water distribution. As shown in Figure 6, a radiation of 1kW/m² is provided, resulting in 1.9 kWp generated by GPV array using the MPPT controller based FLC. The power and the current of the GPV in Figures 6(a) and 6(b) rapidly go up from transient to steady state and remain stable at max values with an optimum duty cycle of the chopper. In turn, the PV voltage follows its maximum value as shown in Figure 6(c) which shows the good performance of FLC. Concerning Figure 7(a), after a transitory spike, the electromagnetic torque drops almost instantly to a constant amount in steady state with some oscillations and in Figure 7(b) the decrease of torque is slower and therefore it is clear that the SMC efficacy in term of response time is faster than AWIP. Figures 7(c), 7(d) and 7(e) show respectively the IM speed, the water flow and the hydraulic power for both techniques. The speed behavior obtained using FDTC with SMC takes 0.3s to reach the reference without overshooting while the FDTC technique with AWIP takes almost 0.75 s. As consequence, there is a noticeable improvement in response time in water flow and hydraulic power. Figure 7(f) shows the stator flux behavior, which closely follows the reference 1 Wb. Taking a period from the steady state, the stator flux THD value is 17.28% Figure 7(g). Next, a sudden change of PV irradiance level is applied at 1.4s, the radiation level is varied from 0.7 to 1 kW/m² just to confirm the robustness of the proposed controllers.

Table 2. PV DIMEL parameters

Electrical characteristics	
Maximum Power (P _{max})	190 W
Voltage (V _{mp})	30.40 V
Current (I _{mp})	6.25 V
Open-circuit voltage (V _{oc})	36.2 V
Short-circuit current (I _{sc})	6.7 A

Table 3. The boost parameters

Parameters	
PV array voltage (V_{pv})	150 V
DC link voltage (V_{dc})	410 V
switching frequency (f)	4 KHz
boost convert duty ratio (D)	$D = 1 - \frac{V_{pv}}{V_{dc}} = 0.63$
inductance (L)	$L = \frac{D(1-D)^2 \cdot R}{2 \cdot f_s} = 0.172mH$
capacitance (C)	$C = \frac{D}{2 \cdot f_s \cdot R} = 4.92 \mu F$

Table 4. IM parameters

Parameters	Values	Parameters	Values
Power (P_N)	1500 W	Rotor resistance (R_r)	4.282 Ω
Voltage (V_N)	230/400 V	Stator Inductance (L_s)	0.4640 H
Current (I_N)	3.2/5.5 A	Rotor Inductance (L_r)	0.4640 H
Speed (n_N)	1435 rpm	Mutual Inductance (M)	0.4410 H
Frequency (F)	50 HZ	Inertia's moment	0.005 Kg.m ²
Pair Pole (P)	2	Viscous friction coefficient	0.003 N.m.s/rad
Stator resistance (R_s)	5.717 Ω		

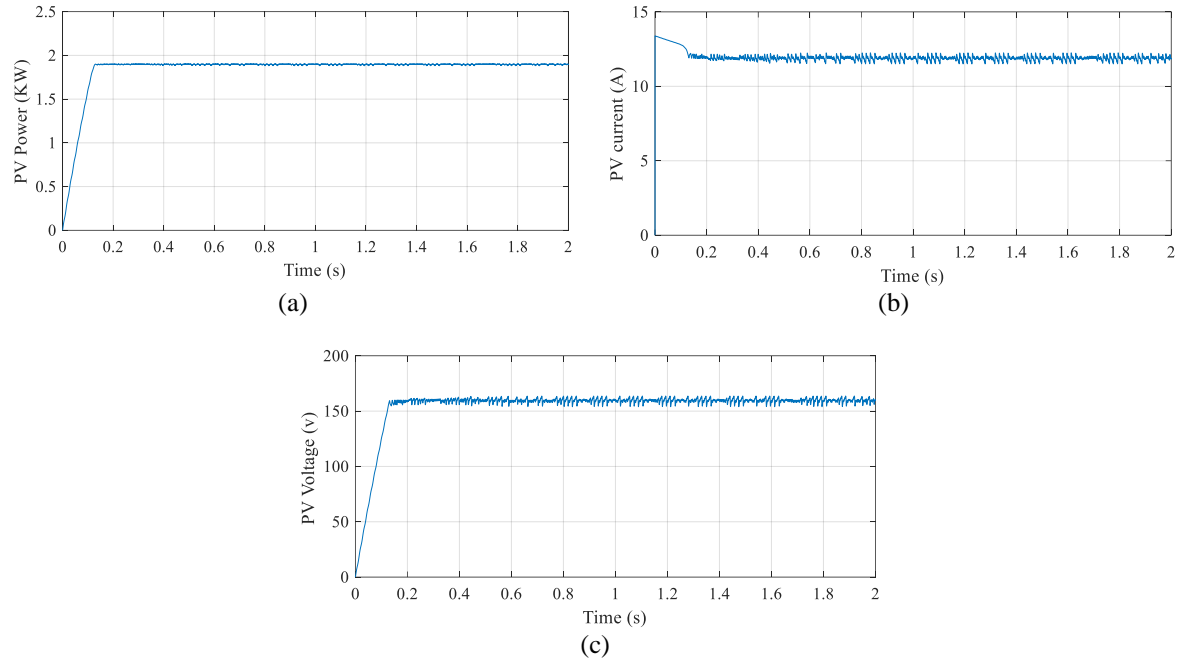


Figure 6. Response of GPV (a) power, (b) current, and (c) voltage

The IM drive's reference speed varies depending on the output power of the PVG which is used to compute the optimal speed, which is then used as a reference speed for the motor-pump. Figures 8(a), 8(b) and 8(c) show the response of a PV array, where the MPPT controls perfectly the power and current values and extracts them from the GPV while the changes in irradiance concerning the voltage is negligible. Figure 9(a) shows the DC voltage while Figures 9(b) and 9(c) illustrate the developed IM electromagnetic torque and the pump torque using both methods. The torque of the PVPS controlled by the FDTC technique with SMC quickly achieves a steady state compared to the PV system controlled by the FDTC with AWIP. The FDTC has however ensured that for variable irradiance, the torque of the motor is equal to that of the pump's need. In regarding the speed response in Figure 9(d), it is worth noting that the good speed tracking has also resulted in good tracking of the PVG power, resulting in maximum power transfer to the water pump. As it can be noticed as well from Figures 9(e) and 9(f) that when the insolation increases, the hydraulic power and the flow rate increase. Figure 9(g) shows the stator flux behavior, which closely follows the reference 1Wb whatever the radiation change. As a result, the performance of the control techniques is evident, they improve the PVPS's performance and robustness, however the SMC outperforms other technique in terms of fast response without overshooting. According to the simulation results, the proposed technique which relies on the association of SMC and FLC increases accuracy in terms of overshoot reduction and response time improvement, and using FLC for MPPT was the best choice to ensure that the proposed system runs smoothly as it appears clearly in results.

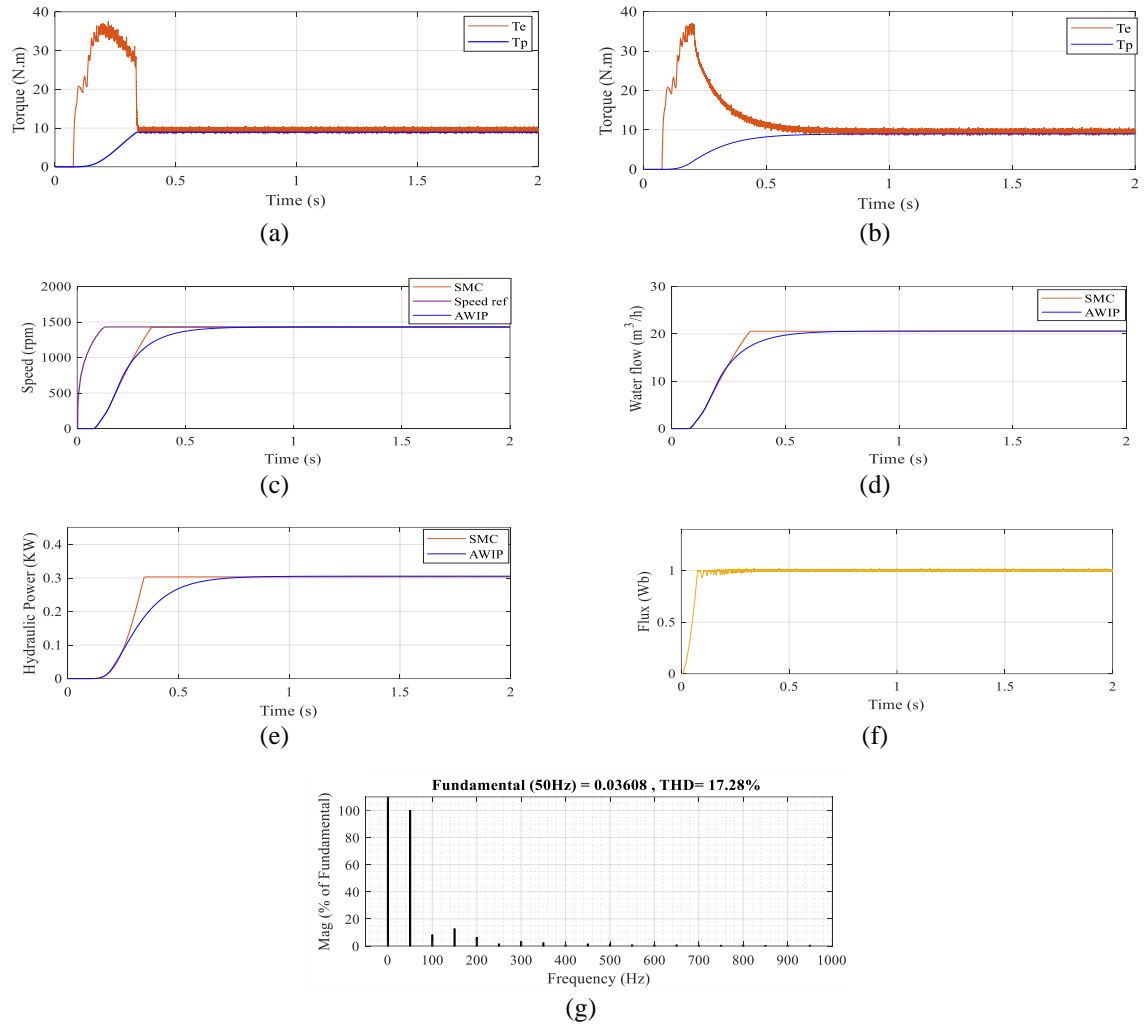


Figure 7. IM response (a) electromagnetic torque and the pump torque with SMC, (b) electromagnetic torque and the pump torque with AWIP(c) IM speed, (d) water flow, (e) hydraulic power(f) stator flux, and (g) FFT analysis of stator flux

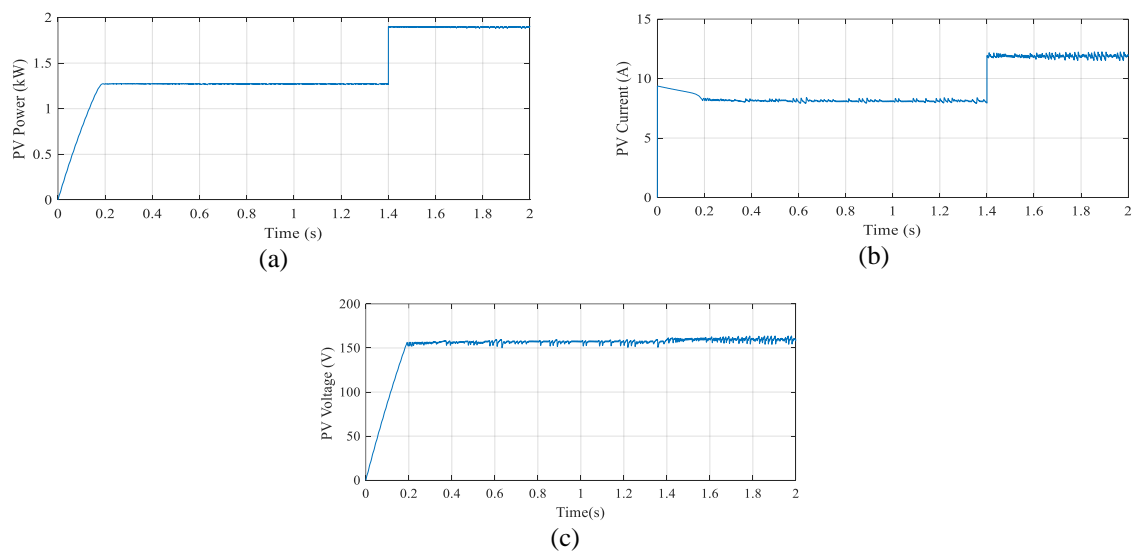


Figure 8. Response of GPV under change radiation (0.7 to 1 KW) (a) power, (b) current, and (c) voltage

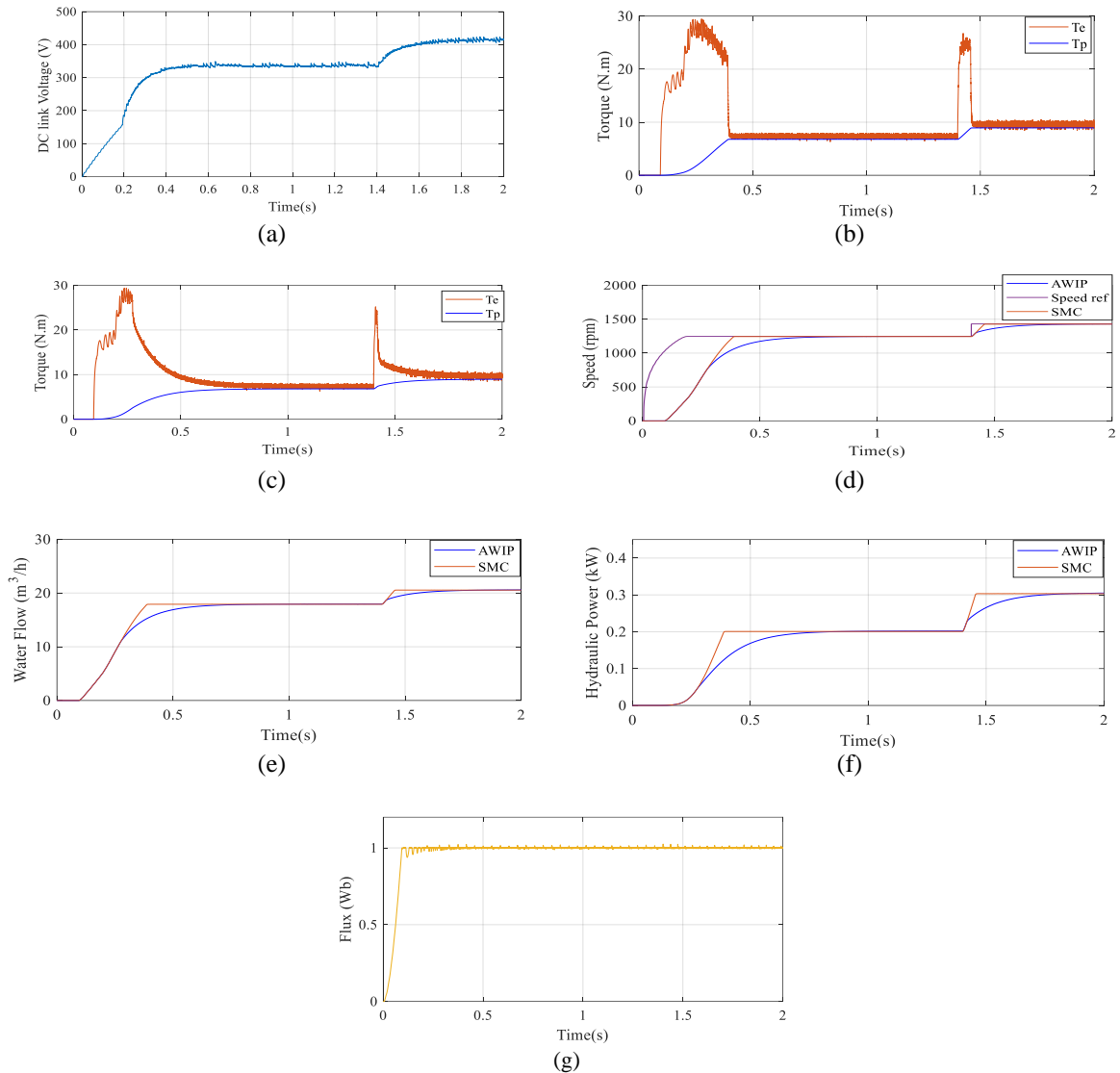


Figure 9. IM response using FDTC (a) DC voltage, (b) electromagnetic torque and the pump torque with SMC, (c) electromagnetic torque and the pump torque with AWIP (d) IM speed, (e) water flow, (f) hydraulic power, and (g) stator flux

5. CONCLUSION




A proposed control for a PV water pumping system is detailed which combines the FDTC and SMC concepts. The main goal is to preserve the PVPS hydraulic parameters at its highest level particularly the water flow while maintaining good and fast performance adapting to all circumstances. The use of MATLAB made it possible to simulate the system after having designed and modeled it, so that the results obtained verify the proposed control and improve it. The adoption of FDTC-based SMC has enhanced the water flow and hydraulic power even at sudden change of PV irradiance. The simulation findings verify the proposed system's design and performance, demonstrating that the SMC is advantageous in IM drive speed regulation and that FLC for MPPT enhances PV pumping system efficiency.

REFERENCES




- [1] S. E. Boukebbous, K. Djallel, N. E. Benbaha, A. Hachemi, and B. Abdelkader, "Effet de l'ombrage sur un système de pompe photovoltaïque," *International Journal of Scientific Research & Engineering Technology*, pp. 14-20, 2016.
- [2] K. Meah, S. Fletcher, and S. Ula, "Solar photovoltaic water pumping for remote locations," *Renewable and Sustainable Energy Reviews*, vol. 12, no. 2, pp. 472-487, 2008. doi: 10.1016/j.rser.2006.10.008.
- [3] B. Singh, A. K. Mishra, and R. Kumar, "Solar Powered Water Pumping System Employing Switched Reluctance Motor Drive," in *IEEE Transactions on Industry Applications*, vol. 52, no. 5, pp. 3949-3957, 2016, doi: 10.1109/tia.2016.2564945.

- [4] N. H. Selman and J. R. Mahmood, "Comparison Between Perturb & Observe, Incremental Conductance and Fuzzy Logic MPPT Techniques at Different Weather Conditions," *International Journal of Innovative Research in Science, Engineering and Technology*, vol. 5, no. 7, pp. 12556–12569, 2016, doi:10.15680/ijirset.2016.0507069.
- [5] E. Kandemir, S. Borekci, and N. S. Cetin, "Comparative analysis of reduced-rule compressed fuzzy logic control and incremental conductance MPPT methods," *Journal of Electronic Materials*, vol. 47, no. 8, pp. 4463–4474, 2018, doi: 10.1007/s11664-018-6273-y.
- [6] J. V. M. Caracas, G. D. C. Farias, L. F. M. Teixeira, and L. A. D. S. Ribeiro, "Implementation of a High-Efficiency, High-Lifetime, and Low-Cost Converter for an Autonomous Photovoltaic Water Pumping System," *IEEE Transactions on Industry Applications*, vol. 50, no. 1, pp. 631–641, 2014, doi: 10.1109/tia.2013.2271214.
- [7] I. M. Alsofyani and N. R. N. Idris, "Simple Flux Regulation for Improving State Estimation at Very Low and Zero Speed of a Speed Sensorless Direct Torque Control of an Induction Motor," *IEEE Transactions on Power Electronics*, vol. 31, no. 4, pp. 3027–3035, 2016, doi: 10.1109/TPEL.2015.2447731.
- [8] A. Achour, D. Rekioua, A. Mohammadi, Z. Mokrani, T. Rekioua and S.Bacha, "Application of Direct Torque Control to a Photovoltaic Pumping System with Sliding-mode Control Optimization," *Electric Power Components and Systems*, vol. 44, no. 2, pp. 172–184, 2015, doi: 10.1080/15325008.2015.1102182.
- [9] C. Moulay-Idriss and B. Mohamed, "Application of the DTC control in the Photovoltaic Pumping System," *Energy Conversion and Management*, vol. 65, pp. 655–662, 2013, doi: 10.1016/j.enconman.2011.08.026.
- [10] M. Errouha, A. Derouich, N. E. Ouanjli and S. Motahhir, "High-Performance Standalone Photovoltaic Water Pumping System Using Induction Motor," *International Journal of Photoenergy*, vol. 2020, pp. 1–13, 2020, doi: 10.1155/2020/3872529.
- [11] M. Errouha, S. Motahhir, Q. Combe, and A. Derouich, "Intelligent control of induction motor for photovoltaic water pumping system," *SN Applied Sciences*, vol. 3, no. 9, pp. 1–14, 2021, doi: 10.1007/s42452-021-04757-4.
- [12] S. E. Daoudi, L. Lazrak, and M. A. Lafkih, "Sliding mode approach applied to sensorless direct torque control of cage asynchronous motor via multi-level inverter," *Protection and Control of Modern Power Systems*, vol. 5, no. 1, pp. 1–10, 2020, doi: 10.1186/s41601-020-00159-7
- [13] W. V. Jones, "Motor Selection Made Easy: Choosing the Right Motor for Centrifugal Pump Applications," *IEEE Industry Applications Magazine*, vol. 19, no. 6, pp. 36–45, 2013, doi: 10.1109/mias.2012.2215649.
- [14] H.Shahinzadeh, M. M.Najaf Abadi, M.Hajahmadi and A. Paknejad, "Design and economic study for use the photovoltaic systems for Electricity Supply in Isfahan Museum Park," *International Journal of Power Electronics and Drive Systems*, vol. 3, no. 1, 2013, doi: 10.11591/ijpeds.v3i1.1797.
- [15] A. Ammar, A. Bourek, and A. Benakcha, "Robust SVM-direct torque control of induction motor based on sliding mode controller and sliding mode observer," *Frontiers in Energy*, vol. 14, no. 4, pp. 836–849, 2017, doi: 10.1007/s11708-017-0444-z.
- [16] A. Braunstein and A. Kornfeld, "Analysis of solar powered electric water pumps," *Solar Energy*, vol. 27, no. 3, pp. 235–240, 1981, doi: 10.1016/0038-092x(81)90124-9.
- [17] K. Rahrah, D. Rekioua, T. Rekioua, and S. Bacha, "Photovoltaic pumping system in Bejaia climate with battery storage," *International Journal of Hydrogen Energy*, vol. 40, no. 39, pp. 13665–13675, 2015, doi: 10.1016/j.ijhydene.2015.04.048.
- [18] R. Kumar and B.Singh, "Brushless DC motor-driven grid-interfaced solar water pumping system," *IET Power Electronics*, vol. 11, no. 12, pp. 1875–1885, 2018, doi: 10.1049/iet-pel.2017.0812.
- [19] M. Arrouf and S. Ghabrour, "Modelling and simulation of a pumping system fed by photovoltaic generator within the Matlab/Simulink programming environment," *Desalination*, vol. 109, no. 1-3, pp. 23–30, 2007, doi: 10.1016/j.desal.2007.04.004.
- [20] A. Mellit and S. A. Kalogirou, "Artificial intelligence techniques for photovoltaic applications: A review," *Progress in Energy and Combustion Science*, vol. 34, no. 5, pp. 574–632, 2008, doi: 10.1016/j.pecs.2008.01.001.
- [21] C. B. Salah and M. Ouali, "Comparison of fuzzy logic and neural network in maximum power point tracker for PV systems," *Electric Power Systems Research*, vol. 81, no. 1, pp. 43–50, 2011, doi: 10.1016/j.epr.2010.07.005.
- [22] A. Chaithanakulwat, "Track the maximum power of a photovoltaic to control a Cascade Five-level inverter a single-phase grid-connected with a fuzzy logic control," *International Journal of Power Electronics and Drive Systems*, vol. 10, no. 4, pp. 1863–1874, 2019, doi: 10.11591/ijpeds.v10.i4.pp1863-1874.
- [23] Y. E. Mourabit, A. E. Derouich, A. E. Ghzizal, N. Ouanjli, and O.Zamzoum, "DTC-SVM Control for Permanent Magnet Synchronous Generator based Variable Speed Wind Turbine," *International Journal of Power Electronics and Drive Systems*, vol. 8, no. 4, pp.1732-1743, 2017, doi: 10.11591/ijpeds.v8.i4.pp1732-1743.
- [24] H, Sudheer, S. F. Kodad, and B. Sarvesh, "Improvements in direct torque control of induction motor for wide range of speed operation using fuzzy logic," *Journal of Electrical Systems and Information Technology*, vol. 5, no. 3, pp. 813–828, 2018, doi: 10.1016/j.jesit.2016.12.015.
- [25] S. E. Daoudi, L. Lazrak, N. E. Ouanjli, and M. A. Lafkih, "Sensorless fuzzy direct torque control of induction motor with sliding mode speed controller," *Computers and Electrical Engineering*, vol. 96, p. 107490, 2021, doi: 10.1016/j.compeleceng.2021.107490.
- [26] N. E. Ouanjli, A. Derouich, A. E. Ghzizal, A. Chebabhi, M. Taoussi, and B. Bossoufi, "Direct Torque Control Strategy Based on Fuzzy Logic Controller for a Doubly Fed Induction Motor," *IOP Conference Series: Earth and Environmental Science*, vol. 161, pp. 012004, 2018, doi: 10.1088/1755-1315/161/1/012004.
- [27] W. Ayri, M. Ourahou, B .E. Hassouni, and A.Haddi, "Direct torque control improvement of a variable speed DFIG based on a fuzzy inference system," *Mathematics and Computers in Simulation*, vol. 167, pp. 308–324, 2020, doi: 10.1016/j.matcom.2018.05.014.
- [28] N. E. Ouanjli, S. Motahhir, A. Derouich, A. E. Ghzizal, A. Chebabhi, and M. Taoussi, "Improved DTC strategy of doubly fed induction motor using fuzzy logic controller," *Energy Reports*, vol. 5, pp. 271–279, 2019, doi: 10.1016/j.egyr.2019.02.001.
- [29] X.-L. Li, J.-G. Parkand, and H.-B. Shin, "Comparison and Evaluation of Anti-Windup PI Controllers," *Journal of Power Electronics*, vol. 11, no. 1, pp. 45–50, 2011, doi: 10.6113/jpe.2011.11.1.045.
- [30] M. Horch, A. Boumediène, and L. Baghli, "Direct torque control of induction machine drive based on sliding mode controller and a stator resistance compensator with a new hybrid observer," *International Journal of Digital Signals and Smart Systems*, vol. 3, no.1/2/3, pp.60, 2019, doi:10.1504/ijds.2019.103384.
- [31] A. Belgacem, Y. Miloud, M. Mostefai, and F. Belgacem, "Direct Torque Control based Slide Mode Control applied to Induction Motor drive in a photovoltaic pumping system," *International Conference on Engineering & MIS*, 2021, pp. 1-6, 2021, doi: 10.1145/3492547.3492756.




BIOGRAPHIES OF AUTHORS

Aicha Belgacem    is Ph.D student in the Department of Electrotechnics Engineering at the university Dr Moulay Tahar of Saida, Algeria. She received BS degree in Electro-technical engineering in 2017 and Master degree in Industrial electrical engineering in 2019. His main research interests revolve around renewable energy concerning photovoltaic water pumping systems. She can be contacted at email: aicha.belgacem95@yahoo.com.






Yahia Miloud    received the B.Eng degree from Bradford University, UK in 1980, the M.Sc degree from Aston University in Birmingham, UK in 1981 and the Ph.D degree from Electrical Machines Department of Electrical and Electronic Engineering, University of Oran (U.S.T.O),Algeria in 2006. From 1982 to 1988 he was as senior Engineer for Sonatrach LNG1 plant, Arzew Algeria where he was in charge of the method section of the maintenance department and responsible for the operation of all UPS of the plant. In 1988 he joined the department of Electrotechnics at the university of Saïda, Algeria where he is still working as a senior lecturer. His main area of research includes power electronics, intelligent control of ac drives and PV systems. He can be contacted at email: miloudyahiaz@yahoo.fr.



Mohamed Mostefai    obtained his BS in electrotechnical engineering in 1994, the MS degree in 2000 and the Ph.D degree in 2009 from the electrotechnical Engineering Institute of The University Science and Technology of Oran USTO Algeria. He is presently professor at the same University. His activities are in photovoltaic and machine drive. He can be contacted at email: mostefaimed@yahoo.fr.



Fatima Belgacem    is Ph.D student in the Department of Electrotechnics Engineering at the university Dr Moulay Tahar of Saida, Algeria. She received BS degree in Electro-technical engineering in 2017 and Master degree in Industrial electrical engineering in 2019. His main research interests revolve around renewable energy concerning photovoltaic photovoltaic water pumping systems. She can be contacted at email: fatima.belgacem95@yahoo.com.